Title
Hydrolysis of Prostaglandin Glycerol Esters by the Endocannabinoid-Hydrolyzing Enzymes, Monoacylglycerol Lipase and Fatty Acid Amide Hydrolase †

Journal
Biochemistry, 46(33)

ISSN
0006-2960

Authors
Vila, Andrew
Rosengarth, Anja
Piomelli, Daniele
et al.

Publication Date
2007-08-01

DOI
10.1021/bi7005898

Hydrolysis of Prostaglandin Glycerol Esters by the Endocannabinoid-Hydrolyzing Enzymes, Monoacylglycerol Lipase and Fatty Acid Amide Hydrolase[†]

Andrew Vila,[‡] Anja Rosengarth,[§] Daniele Piomelli,[||] Benjamin Cravatt,[⊥] and Lawrence J. Marnett*,[‡]

A. B. Hancock Jr. Memorial Laboratory for Cancer Research, Departments of Biochemistry, Chemistry, and Pharmacology, Vanderbilt Institute of Chemical Biology, Center in Molecular Toxicology, and Vanderbilt-Ingram Cancer Center, Vanderbilt University School of Medicine, Nashville, Tennessee 37232-0146, Department of Molecular Biology and Biochemistry, University of California, Irvine, California 92697-4260, Departments of Pharmacology and Biological Chemistry, University of California, Irvine, California 92697-4260, and Departments of Cell Biology and Chemistry, Skaggs Institute for Chemical Biology, The Scripps Research Institute, BCC 159, 10550 North Torrey Pines Road, La Jolla, California 92037

Received March 27, 2007; Revised Manuscript Received June 11, 2007

ABSTRACT: Cyclooxygenase-2 (COX-2) can oxygenate the endocannabinoids, arachidonyl ethanolamide (AEA) and 2-arachidonylglycerol (2-AG), to prostaglandin-H_2-ethanolamide (PGH_2-EA) and -glycerol ester (PGH_2-G), respectively. Further metabolism of PGH_2-EA and PGH_2-G by prostaglandin synthases produces a variety of prostaglandin-EA's and prostaglandin-G's nearly as diverse as those derived from arachidonic acid. Thus, COX-2 may regulate endocannabinoid levels in neurons during retrograde signaling or produce novel endocannabinoid metabolites for receptor activation. Endocannabinoid-metabolizing enzymes are important regulators of their action, so we tested whether PG-G levels may be regulated by monoacylglycerol lipase (MGL) and fatty acid amide hydrolase (FAAH). We found that PG-Gs are poor substrates for purified MGL and FAAH compared to 2-AG and/or AEA. Determination of substrate specificity demonstrates a 30−100- and 150−200-fold preference of MGL and FAAH for 2-AG over PG-Gs, respectively. The substrate specificity of AEA compared to those of PG-Gs was ∼200−300 fold higher for FAAH. Thus, PG-Gs are poor substrates for the major endocannabinoid-degrading enzymes, MGL and FAAH.

COX-2 can oxygenate arachidonylethanolamide (AEA)[1] and 2-arachidonylglycerol (2-AG) to prostaglandin-H_2-ethanolamide (PGH_2-EA) and -glycerol ester (PGH_2-G), respectively (*1*, *2*). Prostaglandin isomerases/synthases metabolize the PGH_2-derived species to the corresponding PGE_2, PGD_2, $PGF_{2\alpha}$, and PGI_2, (but not TxA_2) ethanolamides or glyceryl esters in vitro (*3*). Peritoneal macrophages synthesize PGE_2-G and PGI_2-G in response to zymosan treatment, and RAW 264.7 cells synthesize PGD_2-G when exposed to ionomycin following lipopolysaccharide and interferon-γ pretreatment (*4*, *5*). An important consideration when assessing the impact of PG-G synthesis in cells or tissues is the rate of degradation of this bioactive lipid. For example, primary macrophages do not significantly degrade PG-Gs over several hours, but PGE_2-G is rapidly metabolized to its free acid species in rat plasma [$t_{1/2} \sim 14$ s (*6*)]. In contrast to PG-Gs, PG-EAs are relatively stable to hydrolysis in rat whole blood (*6*). Instead, PGE_2-EA undergoes slow dehydration and/or isomerization to produce PGB_2-EA (approximately two-thirds of the starting material converted over 40 h at 37 °C) (*6*).

Although previous cellular studies demonstrate PG-G formation (*4*, *5*), evidence for the production of these species in intact tissue is lacking. However, it has been shown that COX-2 participates in regulating 2-AG levels in neurons during retrograde signaling (*7*), and COX-2 metabolites of 2-AG metabolism (PGE_2-G, D_2-G, and $F_{2\alpha}$-G) increase the frequency of miniature inhibitory postsynaptic currents in primary hippocampal neurons (*8*). This latter effect is independent of endocannabinoid and prostanoid signaling pathways. However, it appears that COX-2 inhibitors specifically block inhibitory retrograde signaling in the hippocampus. Others show that COX-2 does not contribute to the regulation of 2-AG levels during inhibitory or excitatory retrograde signaling in mouse cerebellum or hippocampus, respectively (*9*, *10*). Characterization of the enzymatic activity responsible for PG-G degradation could be important in explaining the potential biological function of PG-Gs. Also, identification of an enzyme or enzymes that degrade PG-Gs would allow specific targeting of esterases that recognize these species. Therefore, an accurate model of PG-G synthesis and biological function could be assessed.

Two enzymes that may participate in the degradation of PG-Gs include monoacylglycerol lipase (MGL) and fatty acid

[†] This work was supported by research grants from the National Institutes of Health (GM15431, DA-12413, and DA-12447).

* To whom correspondence should be addressed. E-mail: larry.marnett@vanderbilt.edu. Phone: (615) 343-7329. Fax: (615) 343-7534.

[‡] Vanderbilt University School of Medicine.

[§] Department of Molecular Biology and Biochemistry, University of California.

[||] Departments of Pharmacology and Biological Chemistry, University of California.

[⊥] The Scripps Research Institute.

[1] Abbreviations: COX-2, cyclooxygenase-2; AEA, arachidonyl ethanolamide (anandamide); AG, arachidonylglycerol; EA, ethanolamide; PG, prostaglandin; MGL, monoacylglycerol lipase; FAAH, fatty acid amide hydrolase; 2-OG, 2-oleoylglycerol; ELSD, evaporative light scattering detection; MS, mass spectrometry.

10.1021/bi7005898 CCC: $37.00
Published on Web 07/25/2007

amide hydrolase (FAAH). MGL is responsible for the degradation of monoacylglycerols, such as 2-AG, in the brain (*11*). FAAH degrades *N*-acyl ethanolamides such as AEA but also degrades 2-AG in vitro (*12*). Both of these hydrolase enzymes regulate the levels of endocannabinoids (2-AG and AEA) during retrograde synaptic signaling in the hippocampus (*7*, *13*). Recently, it was reported that the COX products of 2-AG and AEA only slightly inhibit degradation of 2-oleoylglycerol (2-OG) and AEA by cytosolic (MGL-containing) and membrane (FAAH-containing) fractions isolated from rat brain cerebellum, respectively (*14*). Similarly, another study showed that the ethanolamide derivatives of PGE_2, PGD_2, and $PGF_{2\alpha}$ were unable to inhibit AEA hydrolysis by FAAH activity (*15*). Therefore, PG-Gs and PG-EAs may weakly interact with MGL and FAAH. This study evaluates the ability of MGL and FAAH to degrade PG-Gs in vitro. The hydrolysis of PG-Gs was tested with purified MGL and FAAH, and the efficiency of catalysis for PG-Gs was shown to be much lower compared to that of 2-AG and/or AEA.

MATERIALS AND METHODS

Materials. PGE_2, PGE_2-d_4, PGD_2, $PGF_{2\alpha}$, PGE_2-G, PGD_2-G, $PGF_{2\alpha}$-G, PGE_2-EA, PGD_2-EA, $PGF_{2\alpha}$-EA, 2-AG, AEA, AA, and dihomolinolenic acid (LLA) were obtained from Cayman Chemical Co. (Ann Arbor, MI). PGE_2-G-d_5 was synthesized as described previously (*2*). HPLC solvents were purchased from Fisher Scientific (Chicago, IL). PEEK tubing and fittings were purchased from Upchurch Scientific (Oak Harbor, WA). Rat brain MGL was cloned and expressed in COS-7 cells (*16*) and purified in the Piomelli laboratory. Rat liver FAAH was expressed in *Escherichia coli* and purified as described previously in the Cravatt laboratory (*17*). A Luna C18 column (10 cm × 2.0 mm, 3 μm particle size) was obtained from Phenomenex (Torrance, CA). HLB oasis columns were from Waters Chromatography (Milford, MA).

PGE_2-G, 2-AG, and AEA Hydrolysis Assay. Hydrolysis of PGE_2-G, PGD_2-G, $PGF_{2\alpha}$-G, and 2-AG by purified rat brain MGL was assayed in 50 mM potassium phosphate (pH 8.0) as described previously (*18*). MGL was incubated at 37 °C for 2 min prior to the addition of substrates. All substrates were prepared as 100× stock solutions in MeOH and diluted to 1% (v/v) in 500 μL of reaction mixture. MGL concentration-dependent hydrolysis of 50 μM 2-AG or PGE_2-G was assessed with 0.35−3.5 μg/mL MGL in 500 μL at time points of 0, 5, 10, and 30 min at 37 °C. Substrate concentration-dependent hydrolysis rates were determined with 2−100 μM 2-AG and 25−400 μM PGE_2-G using 0.35 and 0.7 μg/mL MGL, respectively. Time points for the substrate concentration dependence with MGL were 30 min for 2-AG and 60 min for PGE_2-G (both hydrolysis rates were linear up to these time points). Samples containing 2-AG were quenched with 1 volume of an ice-cold $CHCl_3$/MeOH solution (2:1, v:v) containing 10 μM butylated hydroxyanisole (BHA, Sigma, St. Louis, MO.). BHA was added to minimize autoxidation of polyunsaturated fatty acid chains of 2-AG, AEA, AA, and LLA. For 0 min time points, substrate was added to reaction buffer containing 1 volume of $CHCl_3$/MeOH (2:1, v:v) on ice. LLA (25 nmol per reaction; 50 μM final concentration) was added as an internal standard to quantify formation of AA from 2-AG hydrolysis. Distilled H_2O (250 μL) was added followed by vortexing and centrifugation (2500 rpm for 2 min). The lower phase was removed, and the upper phase was reextracted with 500 μL of chloroform. The extract was dried under argon and then redissolved in 100 μL of a distilled H_2O/MeOH mixture (3:7, v:v) for HPLC−UV analysis.

Reactions that included PG-Gs were quenched with addition of 1.6 volumes of ice-cold 20 mM ammonium acetate (pH 4.0). The samples were then loaded onto HLB Oasis columns (30 mg capacity; Waters) and washed successively with 1 mL each of 0.2% aqueous acetic acid and 0.2% aqueous acetic acid with 10% MeOH, and then PG-Gs and PGs were eluted with 1 mL of 100% MeOH. The extracts were dried under argon, redissolved in 100 μL of a distilled H_2O/MeOH mixture (7:3, v:v), and analyzed by HPLC with evaporative light scattering detection (ELSD) as described below. Quantification of PG-Gs was carried out relative to the appropriate internal standard (e.g., PGE_2-EA was used for PGE_2-G). PGD_2 was used as an internal standard for PGE_2 and $PGF_{2\alpha}$ quantification, and PGE_2 was used for an internal standard for PGD_2 quantification. Internal standards in MeOH were added in 10 μL aliquots to quenched reaction mixtures. PG-EA and PG free acid internal standards were added to each reaction mixture (e.g., 25 and 1.25 nmol per reaction and 50 and 2.5 μM for PG-EA and PG free acid, respectively). PG-EAs were used as internal standards because they are stable in brain homogenates that contain FAAH and MGL over several hours. All reactions were performed in triplicate.

Hydrolysis of PG-G, 2-AG, and AEA with FAAH was performed in 125 mM Tris (pH 9.0) and 1 mM EDTA with 0.1% Triton X-100 (v:v) at 37 °C as previously described (*17*). Time points of 0, 5, 10, and 30 min were used to determine FAAH concentration dependence (0.5−25 μg/mL). To determine substrate concentration dependence, 25−1000 μM AEA and 2-AG and 25−2000 μM for PG-Gs were used with 1 μg/mL FAAH. Also, substrate concentration dependence hydrolysis rates for AEA and 2-AG were determined after incubation for 5 min, whereas rates for PG-G hydrolysis were determined after 30 min (both hydrolysis rates were linear up to these time points). 2-AG or AEA was extracted with $CHCl_3$ and MeOH as described above for the MGL assay and analyzed by HPLC−UV, and samples containing PG-Gs were extracted as described above and analyzed by HPLC−ELSD.

Hydrolysis of PG-Gs in RAW 264.7 Cells. RAW 264.7 cells were obtained from the American Type Culture Collection. The cells were maintained in Dulbecco's modified Eagle's medium (DMEM) supplemented with GlutaMax, high glucose, sodium pyruvate, and pyridoxine HCl (Invitrogen, Grand Island, NY) containing 10% heat-inactivated fetal calf serum (FCS) (Atlas, Fort Collins, CO) (DMEM/FCS). Cells at 90% confluency were passaged into 35 mm plates at a density of 5×10^5 cells/mL in 1 mL of DMEM/FCS as previously described (*19*). After incubation for 2 h, 1 mL of DMEM/FCS containing 40 ng/mL GM-CSF was added to each plate for an additional 22 h. Subsequently, the medium was aspirated and 2 mL of fresh DMEM/FCS containing 20 ng/mL GM-CSF, 100 ng/mL lipopolysaccharide, and 10 ng/mL interferon-γ was added. RAW cells were incubated for an additional 5 h followed by aspiration of the medium and two washes with calcium- and magnesium-free phosphate-buffered saline (PBS) (pH 7.4). Fresh DMEM

(1 mL) was added followed by 1 mL of DMEM with 1% DMSO (v:v) containing either 100 nM PGE_2-G or 2 μM 2-AG to start the reaction. The amount of PGE_2-G-d_5 remaining was assayed at 0, 0.5, 1, 2, and 4 h intervals. At each time point, the medium was removed and spiked with deuterated internal standards, $PGF_{2\alpha}$-G-d_5 (50 pmol/mL) and PGE_2-d_4 (50 pmol/mL), and 10 μL of glacial acetic acid. The samples were loaded onto HLB Oasis columns followed by washing and elution steps as described above. Dried samples were redissolved in a distilled H_2O/MeOH mixture (65:35, v:v) and analyzed by HPLC with electrospray ionization tandem mass spectrometry (LC−ESI-MS/MS).

For 2-AG-containing samples, the medium was removed at 0, 5, 10, 20, 30, and 60 min intervals and added to 1 mL of ice-cold acetonitrile (ACN) containing deuterated standards, 2-AG-d_8 (100 ng/mL) and AA-d_8 (10 ng/mL), and 10 μM BHA. Subsequently, RAW cells were scraped into 500 μL of ice-cold MeOH (two times) and added to the same collected medium. The lipids were extracted twice with 5 mL of an ethyl actetate/hexane/acetic acid mixture (9:1:0.01, v:v:v). The sample was dried under argon, redissolved in 1 mL of an ethyl acetate/methanol/acetic acid mixture (95:5:0.1, v:v:v), and loaded onto unconditioned silica Sep-Pak columns from Waters. The same solvent was used to wash the Sep-Pak columns (three times). Both breakthrough and wash fractions then were combined, dried under argon, and redissolved in 100 μL of a distilled H_2O/MeOH mixture (25:75, v:v) for LC−ESI-MS/MS analysis.

URB-602 [a specific MGL inhibitor (*13*)] was used to test whether PGE_2-G-d_5 was a substrate for MGL in intact RAW cells. URB-602 (100 μM) was added to pretreated RAW cells in 1 mL of DMEM with 1% DMSO (v:v) for 15 min. Subsequently, 1 mL of either PGE_2-G-d_5 (100 nM) or 2-AG (2 μM) was added to RAW cells in DMEM for a final concentration of 50 nM or 1 μM, respectively. The amount of 2-AG or PGE_2-G-d_5 remaining was determined in the presence or absence of URB-602 after 1 or 4 h, respectively. All reactions were performed in triplicate.

Metabolism of PGE_2-G in Brain Particulate Fractions. A 10% homogenate of dog brain frontal cortex in lysis buffer [20 mM Tris-HCl buffer (pH 7.5) containing 0.32 M sucrose, 1 mM EDTA, and 2.5 mM DTT] was produced with a polytron homogenizer (model PCU11, VWR, West Chester, PA). Unbroken cells and nuclei were removed by centrifugation (500*g* for 10 min at 4 °C), and the supernatant was recovered as the crude homogenate. The crude homogenate was centrifuged (180000*g* for 50 min at 4 °C), and the pellet was recovered as the particulate fraction. The particulate fraction was then adjusted to 0.1 mg/mL protein in 50 mM potassium phosphate buffer (pH 7.4) and incubated for 15 min at 37 °C with URB-597 (a specific FAAH inhibitor) (0.0001, 0.001, 0.005, 0.500, and 10 μM) or vehicle control (MeOH). Both AEA and PGE_2-G were prepared as 100× stock solutions in MeOH and diluted to 1% (v:v) for final concentrations of 50 and 10 μM, respectively. The amount of PGE_2-G or AEA remaining was determined at 30 min by using HPLC−ELSD or HPLC−UV analysis, respectively (described below). Percent remaining activity was determined at each URB-597 concentration relative to the vehicle control (designated 100% activity). All reactions were performed in triplicate.

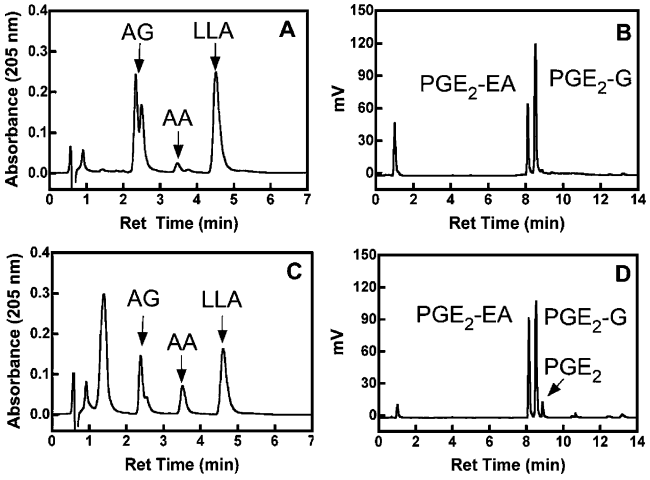

FIGURE 1: MGL degradation of 2-AG and PGE_2-G. Panels A and C represent 2-AG hydrolysis in the absence and presence, respectively, of 0.7 μg/mL MGL after incubation for 10 min. The HPLC chromatograms for panels A and C show 2-AG and 1(3)-AG (2.3 min), AA (3.6 min), and dihomolinolenic acid (LLA) (4.8 min). The peak at 1.5 min in panel C is Triton X-100 from the stock solution of MGL. 2-AG and LLA were both added at 50 μM (5 nmol on column). The amount of AA formed 30 min after the injection was 14.7 μM (1.47 nmol on column). Panels B and D represent PGE_2-G hydrolysis in the presence of 0.7 and 3.5 μg/mL MGL, respectively, after incubation for 30 min. The HPLC chromatograms in panels B and D show PGE_2-EA (8.1 min), PGE_2-G (8.5 min), and PGE_2 (9.0 min). The ELSD drift tube temperature was set to 50 °C; the nitrogen source was set to 2.4 psi, and the gain was set to 6 mV. PGE_2-EA and PGE_2-G were both at 50 μM (5 nmol on column). The levels of PGE_2 formed after 30 min in panels B and D were 3.0 and 8.6 μM, respectively (0.30 and 0.86 nmol on column, respectively).

HPLC Analysis. Analysis of prostanoids was accomplished by reverse-phase (RP) HPLC−ELSD, and endocannabinoid analysis was achieved via RP HPLC−UV. The HPLC system used was a Waters 2695 separation module with an autosampler and pump. Resolution of PG-EAs, PG-Gs, and PGs was afforded by isocratic elution on a Phenomenex Luna C18 column (100 mm × 2.0 mm, 3 μm particle size) at a column temperature of 40 °C. For the assay of PG-G hydrolysis, two different conditions were used. The first condition quantified both the degradation of PGE_2-G and the formation of PGE_2. Solvent A was distilled H_2O with 0.1% acetic acid, and solvent B was ACN with 0.1% acetic acid. The samples were injected onto the column at a solvent composition of 80% A and 20% B with a flow rate of 0.3 mL/min. After a 1 min hold under the same solvent conditions, the level of solvent B was linearly increased from 20 to 50% over 3 min and then held at 50% for an additional 5 min, at which time PGE_2-EA, PGE_2-G, and PGE_2 eluted off the column [8.1, 8.5, and 9.0 min, respectively (Figure 1B,D)]. The ELSD detector drift tube was set to 50 °C and the nitrogen source to 2.4 psi, and the gain was 6 mV. The second condition was used to assess the amount of PG free acid produced as a function of the concentration of the respective PG-G species. The solvent composition was 65:35:0.1 (v:v:v) distilled H_2O:ACN:acetic acid, and the flow rate was 0.3 mL/min. The ELSD detector drift tube and nitrogen source were the same, but the gain was set to 10 mV. PG-EAs eluted at ∼2.3−2.4 min, PG-Gs at ∼3.1−3.5 min, and PGs at 4−5 min (Figure 3A,B). The signal from the ELSD detector is a logarithmic response, so a plot of log(nanograms of com-

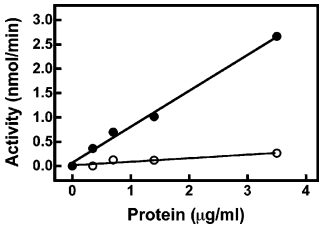

FIGURE 2: Enzyme concentration dependence for hydrolysis of 2-AG and PGE_2-G by MGL. 2-AG (●) or PGE_2-G (○) was incubated with MGL for 0, 5, 10, and 30 min. The samples were extracted and assessed by HPLC−UV analysis for 2-AG hydrolysis or HPLC−ELSD for PGE_2-G hydrolysis as described above. Experiments were performed in triplicate.

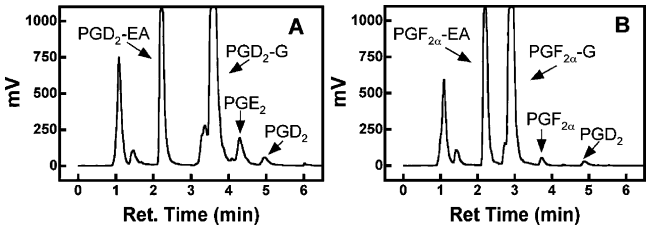

FIGURE 3: HPLC−ELSD chromatograms for MGL-mediated degradation of PGD_2-G and $PGF_{2\alpha}$-G. Panels A and B depict data for 200 μM PGD_2-G and $PGF_{2\alpha}$-G incubated with 0.7 μg/mL MGL for 60 min, respectively. Panel A shows data for PGD_2-G (3.7 min) and its internal standard, PGD_2-EA (2.3 min), and PGD_2 (4.9 min) and its internal standard, PGE_2 (4.3 min). Panel B shows data for $PGF_{2\alpha}$-G (3.0 min) and its internal standard, $PGF_{2\alpha}$-EA (2.2 min), and $PGF_{2\alpha}$ (3.7 min) and its internal standard, PGD_2 (4.9 min). The PG-EA peaks are representative of 50 μM analyte (5 nmol on column) for the corresponding PG-G (100 μM, 10 nmol on column) being studied. The ELSD detector was set to a gain of 10 mV to accurately assess PG free acid formation, which results in the PG-EA and PG-G peaks being off-scale. Panel A shows PGD_2 formation (5.34 μM, 0.53 nmol on column) and panel B $PGF_{2\alpha}$ formation (4.72 μM, 0.47 nmol on column), relative to their respective internal standards of PGE_2 (5 μM, 0.5 nmol on column) and PGD_2, respectively (2.5 μM, 0.25 nmol on column).

pound) versus log(peak area) produces a straight line. The response of the instrument has a dynamic range of approximately 1 order of magnitude. Therefore, the first and second condition had to be done separately with different gain settings. Also, the volumes of injection were changed with the expected sample load of PGs to fall within the dynamic range. For a gain of 10 mV, the dynamic concentration range was 0.04−2 nmol/injection, and for a gain of 6, the dynamic concentration range was 0.2−10 nmol/injection.

Separation of AEA, 2-AG, and AA was afforded by RP-HPLC with the same column described above using an isocratic elution of an ACN/distilled H_2O/acetic acid mixture (75:25:0.1, v:v:v) at 0.7 mL/min. Peaks were detected with a Waters 2487 dual-wavelength absorbance detector set at 205 nm. Arachidonylglycerol eluted as a mixture of the 2- and 1(3)-isomer (Figure 1A) after incubation in aqueous buffer for 30 min. Retention times for AEA, 2- and 1(3)-AG, AA, and LLA were 1.8, 2.3, 3.4, and 4.4 min, respectively (panels A and C of Figure 1 for 2-AG and 1(3)-AG, AA, and LLA, respectively).

HPLC with Tandem Mass Spectrometry. Analysis of endocannabinoids, AA, and prostanoids was accomplished through use of reverse-phase HPLC coupled to electrospray tandem mass spectrometry (LC−ESI-MS/MS) as previously described (*19*, *20*). HPLC separation of endocannabinoids was accomplished with a solvent composition of 70 μM silver acetate in a distilled H_2O/MeOH mixture (15:85, v:v) with a flow rate of 0.3 mL/min on a Phenomenex Luna C18 column (50 mm × 2.0 mm, 3 μm particle size) at a column temperature of 40 °C. Silver ion coordination was used for electrospray ionization of endocannabinoids, resulting in [M + Ag^+] species. The selected reaction monitoring (SRM) *m*/*z* transitions were *m*/*z* 454 → 436 for [AEA + Ag^{107}], *m*/*z* 485 → 411 for [2-AG + Ag^{107}], and *m*/*z* 519 → 412 for [AA^- + 2Ag^+]. Mass spectrometric conditions for 2-AG, AEA, and AA fragmentation were as follows; capillary temperature, 350 °C; capillary offset, 35 V; spray voltage, 5.0 kV; sheath gas, 49 psi; auxiliary gas, 25 psi; CID pressure, 1.5 mTorr; collision energy, 30 V; and tube lens offset, 130 V.

PG-G and PG analytes were separated by HPLC using 2 mM ammonium acetate in distilled H_2O and acetic acid (pH 3.3) and ACN (65:35, v:v) at a flow rate of 0.3 mL/min using the same column conditions described above. The prostanoids coordinate with the NH_4^+ cation, resulting in formation of the [M + NH_4^+] adduct, resulting in addition of 18 mass units. The SRM *m*/*z* transitions for [PGE_2-G-d_5 + NH_4^+], [$PGF_{2\alpha}$-G-d_5 + NH_4^+], [PGE_2-d_4 + NH_4^+], and [PGE_2 + NH_4^+] were *m*/*z* 449 → 391, *m*/*z* 451 → 393, *m*/*z* 374 → 321, and *m*/*z* 370 → 317, respectively. Mass spectrometric conditions for PG-G and PG fragmentation were as follows; capillary temperature, 300 °C; capillary offset, 35 V; spray voltage, 4.3 kV; sheath gas, 35 psi; auxiliary gas, 21 psi; and CID pressure, 1.0 mTorr. The collision energy was varied from 16 to 22 V and the tube lens offset from ∼80 to 130 V.

RESULTS

Hydrolysis of 2-AG, AEA, PGE_2-G, PGD_2-G, and $PGF_{2\alpha}$-G by MGL. The relative ability of MGL to hydrolyze PG-Gs to 2-AG was assessed by HPLC−ELSD. Panels A and C of Figure 1 demonstrate that approximately 30% of 50 μM 2-AG was converted to AA after incubation for 10 min with 0.7 μg/mL MGL. However, the same concentration of MGL produced a barely detectable level of PGE_2 after incubation for 30 min with 50 μM PGE_2-G (Figure 1B). At the highest concentration of MGL that was tested (3.5 μg/mL), approximately 18% of 50 μM PGE_2-G was hydrolyzed to PGE_2 (Figure 1D). The initial rates of 2-AG hydrolysis compared to that of PGE_2-G as a function of MGL concentration show an ∼10-fold higher value for the former at a constant substrate concentration of 50 μM [740 ± 67.5 nmol of 2-AG min^{-1} (mg of protein)$^{-1}$ vs 74.6 ± 14.7 nmol of PGE_2-G min^{-1} (mg of protein)$^{-1}$ (Figure 2)]. The relative efficiency of hydrolysis of PG-G by MGL compared to that of 2-AG was tested by varying the substrate concentration. For these experiments, 0.7 μg/mL MGL was used to determine PG-G hydrolysis rates, and the time course was extended to 60 min. At 0.7 μg/mL MGL, the hydrolysis rates of PG-Gs were linear through incubation for 60 min. The substrate concentration dependence for 2-AG hydrolysis was determined with 0.35 μg/mL using a reaction time of 30 min. As shown in Figure 3, the percent conversion of PGD_2-G and $PGF_{2\alpha}$-G to their corresponding free acids with MGL was also low. The amount of PG free acid formed at initial substrate concentrations of 25−400 μM ranged from 5 to 1% conversion after incubation for 60 min (data not shown). Nonlinear regression analysis of a plot of the rate of 2-AG hydrolysis

Table 1: Kinetic Parameters for MGL Degradation of 2-AG and PG-Gs[a]

species	k_{cat} (min^{-1})	K_m (μM)	k_{cat}/K_m (μM^{-1} min^{-1})
2-AG	21 ± 2	10 ± 3	2.1
PGE_2-G	9.6 ± 1.5	150 ± 40	6.4×10^{-2}
PGD_2-G	4.1 ± 0.3	133 ± 30	3.1×10^{-2}
$PGF_{2\alpha}$-G	8.6 ± 1.7	311 ± 104	2.7×10^{-2}

[a] 2-AG (2−100 μM) was incubated with 0.35 μg/mL MGL. PGE_2-G, PGD_2-G, or $PGF_{2\alpha}$-G (25−400 μM) was incubated with 0.7 μg/mL MGL. Initial rates were determined for 2-AG and the PG-Gs after incubation for 30 and 60 min, respectively. Initial rates for 2-AG and PG-G degradation were linear throughout the reaction. Samples were extracted as described above and analyzed by HPLC with either UV (2-AG hydrolysis) or ELSD detection (PG-G hydrolysis). The hyperbolic plot of initial rate vs initial concentration was determined with nonlinear regression in Prizm. Experiments were performed in triplicate.

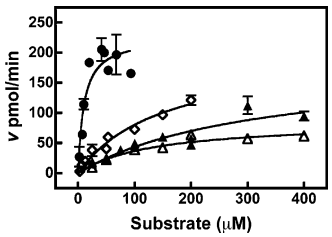

FIGURE 4: Substrate concentration dependence for hydrolysis of PG-G and 2-AG by MGL. 2-AG (●) hydrolysis was evaluated with 0.35 μg/mL MGL, and hydrolysis of PG-Gs [(▲) $PGF_{2\alpha}$-G, (△) PGD_2-G, and (◇) PGE_2-G] was evaluated with 0.7 μg/mL MGL. 2-AG was incubated with MGL for 30 min, and PG-Gs were incubated with MGL for 60 min. Samples were analyzed by HPLC with either UV (2-AG hydrolysis) or ELSD (PG-G hydrolysis) detection, and experiments were performed in triplicate.

with 0.35 μg/mL MGL versus initial 2-AG concentration yielded values of K_m and k_{cat} for the reaction (Table 1). These values are approximate because the critical micellar concentration of 2-AG is 25 μM, making free substrate limiting at higher concentrations (data not shown). PG-Gs (E_2, D_2, and $F_{2\alpha}$) were incubated at concentrations ranging from 25 to 400 μM with 0.7 μg/mL MGL. As shown in Figure 4 and Table 1, k_{cat} values for PG-Gs were much lower (50−80%) than that of 2-AG and the K_m values were much higher (13−30-fold). The high error associated with the K_m values for the PG-G species may be from the lack of complete saturation of MGL. The relative substrate efficiency for MGL was 32−100 times higher for 2-AG (Table 1). There were only small differences in the k_{cat} and K_m values among PG-G species. The k_{cat} for PGE_2-G hydrolysis was ~2-fold higher than those of PGD_2-G and $PGF_{2\alpha}$-G, and the K_m for PGE_2-G was similar to that of PGD_2-G and 2-fold lower than that of $PGF_{2\alpha}$-G (Table 1).

Metabolism of 2-AG, AEA, PGE_2-G, PGD_2-G, and $PGF_{2\alpha}$-G by FAAH. The relative ability of FAAH to degrade PG-Gs relative to those of AEA and 2-AG also was assessed. Comparison of the initial rates of hydrolysis for AEA compared to that of PGE_2-G as a function of FAAH concentration showed a 22-fold higher rate for the former [692 ± 53.9 nmol of AEA min^{-1} (mg of protein)$^{-1}$ vs 31.8 ± 2.6 nmol of PGE_2-G min^{-1} (mg of protein)$^{-1}$ (Figure 5)]. The effect of substrate concentration on PG-G, AEA, and 2-AG hydrolysis with 1 μg/mL FAAH was also tested (Figure 6). The k_{cat} for 2-AG hydrolysis was 2-fold lower than that of AEA, and the K_m for 2-AG was 3-fold higher than that for AEA (Table 2 and Figure 6). The substrate

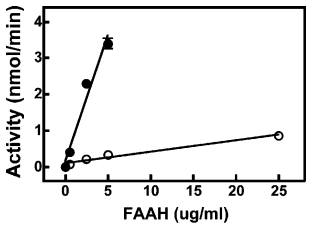

FIGURE 5: Enzyme concentration dependence for hydrolysis of AEA and PGE_2-G by FAAH. AEA at 50 μM (●) or PGE_2-G at 50 μM (○) was incubated with FAAH for 0, 5, 10, and 30 min. Samples were extracted and analyzed by HPLC−UV (AEA hydrolysis) and HPLC−ELSD (PGE_2-G hydrolysis) as described above. Experiments were performed in triplicate.

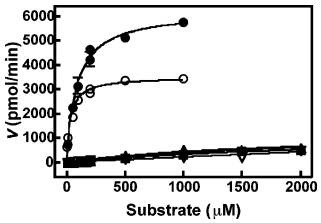

FIGURE 6: Substrate concentration dependence for hydrolysis of PG-G, AEA, and 2-AG by FAAH. FAAH was at 1 μg/mL; concentrations of 2-AG (●) and AEA (○) varied from 25 to 1000 μM, and concentrations of PG-Gs [(▲) $PGF_{2\alpha}$-G, (△) PGD_2-G, and (◇) PGE_2-G] varied from 25 to 2000 μM. 2-AG and AEA were incubated with FAAH for 5 min, and PG-Gs were incubated for 30 min. Experiments were performed in triplicate and analyzed by HPLC with either UV detection or ELSD.

Table 2: Kinetic Paramaters for FAAH Degradation of AEA, 2-AG, and PG-Gs[a]

species	k_{cat} (s^{-1})	K_m (μM)	k_{cat}/K_m (μM^{-1} s^{-1})
2-AG	28 ± 1	89 ± 10	0.31
AEA	16 ± 1	34 ± 4	0.46
PGE_2-G	6.5 ± 1.2	3600 ± 1000	1.8×10^{-3}
PGD_2-G	1.7 ± 0.2	1100 ± 400	1.6×10^{-3}
$PGF_{2\alpha}$-G	4.8 ± 1.1	2400 ± 800	2.0×10^{-3}

[a] The concentration of FAAH was 1 μg/mL with the concentrations of 2-AG and AEA varied from 25 to 1000 μM, and concentrations of $PGF_{2\alpha}$-G, PGD_2-G, and PGE_2-G were varied from 25 to 2000 μM. 2-AG and AEA were incubated with FAAH for 5 min, and PG-Gs were incubated for 30 min. Initial rates for AEA, 2-AG, and PG-G degradation were linear throughout the reaction. Samples were extracted as described above and analyzed by HPLC with either UV (2-AG and AEA hydrolysis) or ELSD (PG-G hydrolysis) detection. The hyperbolic plot of initial rate vs initial concentration was determined with nonlinear regression in Prizm. Experiments were performed in triplicate.

specificity was similar for AEA and 2-AG with k_{cat}/K_m values of 0.462 and 0.313 μM^{-1} s^{-1}, respectively. Estimated k_{cat} values for PGE_2-G, PGD_2-G, and $PGF_{2\alpha}$-G were significantly lower (Table 2 and Figure 6). The high error associated with PG-G k_{cat} values is expected because FAAH was not completely saturated at the highest concentration of PG-Gs that was used. The K_m values for PGE_2-G, PGD_2-G, and $PGF_{2\alpha}$-G were much higher than those for AEA or 2-AG (Table 2). As shown with MGL, it is clear that PG-Gs are poor substrates for FAAH compared to AEA and 2-AG. The estimated k_{cat}/K_m values were 200−300- and 150−200-fold higher for AEA and 2-AG hydrolysis than for PG-Gs (Table 2).

Metabolism of PGE_2-G-d_5 in Intact RAW 264.7 Macrophages by MGL. A specific MGL inhibitor, URB-602 (*13*), was used as a tool to discern whether MGL could metabolize

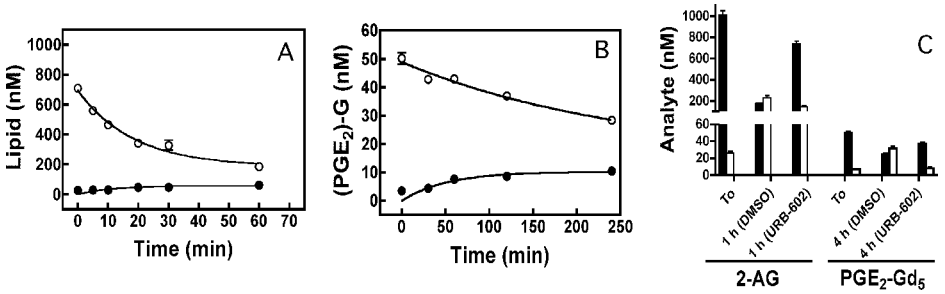

FIGURE 7: Metabolism of PG-Gs in RAW 264.7 cells by MGL in the absence and presence of URB-602. Panel A depicts the degradation of 1000 nM 2-AG (○) with subsequent formation of AA (●). Panel B depicts the degradation of 50 nM PGE_2-G-d_5 (○) with subsequent formation of PGE_2 (●). Panels C shows metabolism of 2-AG and PGE_2-G-d_5 in the presence of URB-602. The left part of the panel, labeled 2-AG, shows 2-AG levels (black bars) and AA levels (white bars) at time zero (T_0), 1 h, and 1 h with URB-602 treatment. The right part of the panel, labeled PGE_2-G-d_5, shows PGE_2-G-d_5 levels (black bars) and PGE_2 levels (white bars) at time zero (T_0), 4 h, and 4 h with URB-602.

PG-Gs in RAW 264.7. These cells were chosen because they make PG-Gs (*4*) and also possess PG-G hydrolytic activity (data not shown). 2-AG (1 μM) and PGE_2-G-d_5 (50 nM) were applied exogenously to RAW 264.7 cells in the presence or absence of 100 μM URB-602. Only 50 nM PGE_2-G-d_5 was added to the RAW cells because it has previously been shown that only nanomole amounts of PG-Gs are produced in macrophages (*4*). The concentrations of 2-AG and PGE_2-G-d_5 given above were chosen because these levels approximate what is produced from endogenous sources following pharmacological challenge. In the absence of URB-602, the RAW cells reduced the concentration of 2-AG to ~18.5 ± 1.1% of its starting value (Figure 7A), and arachidonic acid levels reached ~6% of initial 2-AG levels (61.1 ± 13.3 nM) over a period of 1 h. Arachidonate recovery may not be 100% because of its ability to enter other metabolic pathways (i.e., phospholipid, triacylglycerol synthesis). Degradation of PGE_2-G-d_5 was much slower with ~50% (24.7 ± 1.8 nM) of this species remaining after incubation for 4 h (Figure 7B). The increase in PGE_2 levels accounted for ~42% of the initial PGE_2-G-d_5 concentration (10.4 ± 1.3 nM). As with arachidonic acid, PGE_2 may be subject to further metabolism (i.e., by 15-hydroxyprostaglandin dehydrogenase), thus limiting its recovery. In the presence of 100 μM URB-602, RAW cells reduced the level of exogenously applied 2-AG to ~74.0 ± 4.2% after incubation for 1 h [control levels were ~17.5 ± 0.9% (Figure 7C)]. PGE_2-G-d_5 levels were 37.1 ± 2.4 nM after exposure to URB-602-treated RAW cells for 4 h, whereas those of the control samples were 24.7 ± 1.8 nM (Figure 7C). These results show that there is some inhibition of PGE_2-G hydrolysis in the presence of URB-602 when 2-AG hydrolysis is ~70% inhibited. The total level of hydrolysis of PGE_2-G is much lower than the level of 2-AG hydrolysis. Therefore, 50% inhibition of PGE_2-G hydrolysis with URB-602 accounts for a rather small inhibition of PGE_2-G turnover. The in vitro enzymatic assays show PG-Gs are poor substrates for MGL (~33−100-fold), so it is possible that URB-602 inhibits another PG-G hydrolase to some extent. RAW cells do not possess FAAH protein as judged by Western blot analysis (data not shown), suggesting that these cells do not metabolize PGE_2-G through FAAH enzymatic activity.

Metabolism of PGE_2-G by FAAH Activity in Brain Particulate Fractions. We tested whether FAAH activity from particulate fractions of dog brain frontal cortices degrades PGE_2-G in the presence or absence of a specific FAAH inhibitor, URB-597 (*21*). In the presence of 0.5 μM URB-597, AEA hydrolysis activity was inhibited 75%, whereas PGE_2-G hydrolysis was not significantly inhibited at URB-597 concentrations up to 2.5 μM and was ~30% inhibited at 10 μM (Figure 8). Thus, PGE_2-G appears to be metabolized by an enzymatic activity independent of FAAH in crude brain particulate fractions, and URB-597 appears to modestly inhibit its activity.

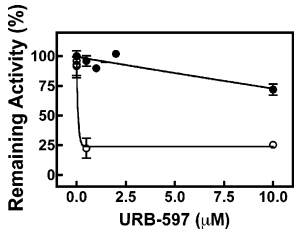

FIGURE 8: Inhibition of PG-G hydrolysis with URB-597 in dog brain particulate fractions. Brain particulate fractions (0.1 mg/mL) were incubated with URB-597 (0.0001−10 μM) for 15 min followed by addition of PGE_2-G (10 μM) or AEA (50 μM). Percent inhibition is the amount of PGE_2-G (●) or AEA (○) hydrolyzed after 30 min compared to vehicle control values (AEA hydrolysis, 21.4 nmol min^{-1} mg^{-1}; and PGE_2-G hydrolysis, 2.92 nmol min^{-1} mg^{-1}).

DISCUSSION

Endocannabinoid hydrolases, MGL and FAAH, were tested for their ability to degrade PG-Gs. Both enzymes hydrolyze 2-AG, the precursor for PG-G from COX-2 oxygenation, very efficiently and are suggested to participate in the rapid inactivation of 2-AG during retrograde signaling. Rat brain MGL hydrolyzes monooleoylglycerol at a rate 5-fold higher than that of 2-AG (*18*). It is estimated that the concentration of 2-AG released during hippocampal retrograde signaling is 10 μM (*18*), which is the K_m for MGL hydrolysis of 2-AG. Recently, a specific MGL inhibitor (URB-602) has been developed as a tool for discerning the role of the enzyme in 2-AG metabolism (*13*). Inclusion of this inhibitor with hippocampal slice preparations significantly extends DSI duration, suggesting that MGL plays an important role in regulating 2-AG levels during retrograde signaling (*13*). Specific inhibitors of COX-2 (e.g., nimesulide and meloxicam) also extend the duration of DSI, suggesting that COX-2 may regulate 2-AG levels (*7*). Another study using primary hippocampal neuron cultures showed that PG-Gs (PGE_2-G, PGD_2-G, and $PGF_{2\alpha}$-G) and PGD_2-EA have

potent effects on retrograde signaling distinct from that of 2-AG (*8*). Although the studies mentioned above suggest that COX-2 is involved in regulating 2-AG levels in the hippocampus, COX-2 inhibitors do not affect inhibitory retrograde signaling in mouse cerebellar slices (*10*) or excitatory signaling in hippocampal slices (*9*). Similar to 2-AG levels, PG-G levels may be tightly regulated by hydrolases during inhibitory retrograde signaling in the hippocampus. The rates of PG-G hydrolysis by MGL were found to be low compared to the rate of 2-AG hydrolysis (the k_{cat}/K_m value is ~30−100-fold lower for the former).

FAAH also degrades 2-AG in addition to AEA, at least in vitro. It has been shown that 2-AG is hydrolyzed at a 4−5-fold higher rate than AEA in recombinant rat, porcine, and cellular FAAH preparations. However, in those studies, the enzyme was not or only partially purified (*22*−*24*). It has since been demonstrated that there is 2-AG hydrolysis activity in particulate fractions of rat brain cerebellum that is independent of FAAH activity (*25*). Microglia cells also contain a novel MGL activity in the mitochondria that is distinct from FAAH (*26*). No comparison of hydrolysis for 2-AG and AEA with purified FAAH has been reported. However, the esterase and amidase activity have been compared. The hydrolysis kinetics of oleoyl methyl ester and oleoyl methyl amine with purified FAAH showed k_{cat} values of 2.8 s^{-1} for the former and 1.9 s^{-1} for the latter. The K_m value for oleoyl methyl ester was 21 μM and for oleoyl methyl amine 9 μM, giving k_{cat}/K_m values of 0.13 and 0.21 μM^{-1} s^{-1}, respectively (*27*). Also, the k_{cat}/K_m values for oleoylethanolamide and monooleoylglycerol were 0.23 and 0.11 μM^{-1} s^{-1}, respectively (*28*). The results of this study show that k_{cat}/K_m values for FAAH hydrolysis of AEA and 2-AG are similar, 0.47 and 0.31 μM^{-1} s^{-1}, respectively. Also, as observed with PG-G degradation with MGL, FAAH activity with PG-Gs is very low compared to that with 2-AG and AEA. Although complete substrate saturation of FAAH by PG-Gs was not reached (up to 2 mM PG-G), the estimated k_{cat}/K_m values are at least 150−200-fold higher for 2-AG hydrolysis and 200−300-fold higher for AEA hydrolysis.

RAW 264.7 cells possess both 2-AG and PG-G hydrolytic activity. Therefore, this cell line was used as an in vivo model to establish that 2-AG and PG-G hydrolytic activities are separate. These studies suggest that MGL contributes little to PGE_2-G hydrolysis in vivo. However, there is some inhibition of PGE_2-G-d_5 hydrolysis in RAW cells treated with URB-602. Although in vitro experiments show that PG-Gs are poor substrates for purified MGL, longer time points (e.g., 4 h) may allow for MGL-mediated PGE_2-G hydrolysis. Alternatively, URB-602 may partially inhibit an unknown lipase/esterase that is responsible for PGE_2-G hydrolysis. Others showed that URB-602 was not a specific MGL inhibitor over FAAH in C6 glioma and RBL2H3 basophilic leukemia cells (*29*). We observed very low FAAH activity in RAW cells under our experimental conditions (data not shown). Therefore, FAAH activity contributed very little to 2-AG degradation. Because FAAH activity in RAW cells was very low, we assumed that these cells do not metabolize PGE_2-G through FAAH enzymatic activity. We used particulate fractions from dog brain cortex to establish that PGE_2-G hydrolysis activity is distinct from AEA hydrolysis activity. When using URB-597 with brain particulate fractions, PGE_2-G hydrolysis is unaffected. Therefore, degradation of PG-Gs occurs in a manner independent of FAAH enzymatic activity from isolated brain particulate fractions.

These results suggest that MGL and FAAH contribute very little to the degradation of PG-Gs in cells. However, it is noteworthy that long chain fatty acyl taurine derivatives are poor substrates for FAAH in vitro, but in vivo experiments using FAAH knockout animals indicate that FAAH plays a major role in their hydrolysis (*28*). Identification of additional enzyme(s) responsible for PG-G degradation could provide important information for inhibitor development or the generation of knockout mice that would represent critical tools for evaluating the biological significance of PG-Gs in vivo.

REFERENCES

1. Yu, M., Ives, D., and Ramesha, C. S. (1997) Synthesis of prostaglandin E2 ethanolamide from anandamide by cyclooxygenase-2, *J. Biol. Chem. 272*, 21181−21186.
2. Kozak, K. R., Rowlinson, S. W., and Marnett, L. J. (2000) Oxygenation of the endocannabinoid, 2-arachidonylglycerol, to glyceryl prostaglandins by cyclooxygenase-2, *J. Biol. Chem. 275*, 33744−33749.
3. Kozak, K. R., Crews, B. C., Morrow, J. D., Wang, L. H., Ma, Y. H., Weinander, R., Jakobsson, P. J., and Marnett, L. J. (2002) Metabolism of the endocannabinoids, 2-arachidonylglycerol and anandamide, into prostaglandin, thromboxane, and prostacyclin glycerol esters and ethanolamides, *J. Biol. Chem. 277*, 44877−44885.
4. Rouzer, C. A., and Marnett, L. J. (2005) Glycerylprostaglandin synthesis by resident peritoneal macrophages in response to a zymosan stimulus, *J. Biol. Chem. 280*, 26690−26700.
5. Rouzer, C. A., and Marnett, L. J. (2005) Structural and functional differences between cyclooxygenases: Fatty acid oxygenases with a critical role in cell signaling, *Biochem. Biophys. Res. Commun. 338*, 34−44.
6. Kozak, K. R., Crews, B. C., Ray, J. L., Tai, H. H., Morrow, J. D., and Marnett, L. J. (2001) Metabolism of prostaglandin glycerol esters and prostaglandin ethanolamides in vitro and in vivo, *J. Biol. Chem. 276*, 36993−36998.
7. Kim, J., and Alger, B. E. (2004) Inhibition of cyclooxygenase-2 potentiates retrograde endocannabinoid effects in hippocampus, *Nat. Neurosci. 7*, 697−698.
8. Sang, N., Zhang, J., and Chen, C. (2006) PGE2 glycerol ester, a COX-2 oxidative metabolite of 2-arachidonoyl glycerol, modulates inhibitory synaptic transmission in mouse hippocampal neurons, *J. Physiol. 572*, 735−745.
9. Straiker, A., and Mackie, K. (2005) Depolarization-induced suppression of excitation in murine autaptic hippocampal neurones, *J. Physiol. 569*, 501−517.
10. Szabo, B., Urbanski, M. J., Bisogno, T., Di Marzo, V., Mendiguren, A., Baer, W. U., and Freiman, I. (2006) Depolarization-induced retrograde synaptic inhibition in the mouse cerebellar cortex is mediated by 2-arachidonoylglycerol, *J. Physiol. 577*, 263−280.
11. Tornqvist, H., and Belfrage, P. (1976) Purification and some properties of a monoacylglycerol-hydrolyzing enzyme of rat adipose tissue, *J. Biol. Chem. 251*, 813−819.
12. Cravatt, B. F., Demarest, K., Patricelli, M. P., Bracey, M. H., Giang, D. K., Martin, B. R., and Lichtman, A. H. (2001) Supersensitivity to anandamide and enhanced endogenous cannabinoid signaling in mice lacking fatty acid amide hydrolase, *Proc. Natl. Acad. Sci. U.S.A. 98*, 9371−9376.
13. Makara, J. K., Mor, M., Fegley, D., Szabo, S. I., Kathuria, S., Astarita, G., Duranti, A., Tontini, A., Tarzia, G., Rivara, S., Freund, T. F., and Piomelli, D. (2005) Selective inhibition of 2-AG hydrolysis enhances endocannabinoid signaling in hippocampus, *Nat. Neurosci. 8*, 1139−1141.
14. Fowler, C. J., and Tiger, G. (2005) Cyclooxygenation of the arachidonoyl side chain of 1-arachidonoylglycerol and related compounds block their ability to prevent anandamide and 2-oleoylglycerol metabolism by rat brain in vitro, *Biochem. Pharmacol. 69*, 1241−1245.
15. Matias, I., Chen, J., De Petrocellis, L., Bisogno, T., Ligresti, A., Fezza, F., Krauss, A. H., Shi, L., Protzman, C. E., Li, C., Liang, Y., Nieves, A. L., Kedzie, K. M., Burk, R. M., Di Marzo, V., and

Woodward, D. F. (2004) Prostaglandin ethanolamides (prostamides): In vitro pharmacology and metabolism, *J. Pharmacol. Exp. Ther. 309*, 745−757.
16. Dinh, T. P., Freund, T. F., and Piomelli, D. (2002) A role for monoglyceride lipase in 2-arachidonoylglycerol inactivation, *Chem. Phys. Lipids 121*, 149−158.
17. Patricelli, M. P., Lashuel, H. A., Giang, D. K., Kelly, J. W., and Cravatt, B. F. (1998) Comparative characterization of a wild type and transmembrane domain-deleted fatty acid amide hydrolase: Identification of the transmembrane domain as a site for oligomerization, *Biochemistry 37*, 15177−15187.
18. Dinh, T. P., Carpenter, D., Leslie, F. M., Freund, T. F., Katona, I., Sensi, S. L., Kathuria, S., and Piomelli, D. (2002) Brain monoglyceride lipase participating in endocannabinoid inactivation, *Proc. Natl. Acad. Sci. U.S.A. 99*, 10819−10824.
19. Kingsley, P. J., Rouzer, C. A., Saleh, S., and Marnett, L. J. (2005) Simultaneous analysis of prostaglandin glyceryl esters and prostaglandins by electrospray tandem mass spectrometry, *Anal. Biochem. 343*, 203−211.
20. Kingsley, P. J., and Marnett, L. J. (2003) Analysis of endocannabinoids by Ag^+ coordination tandem mass spectrometry, *Anal. Biochem. 314*, 8−15.
21. Mor, M., Rivara, S., Lodola, A., Plazzi, P. V., Tarzia, G., Duranti, A., Tontini, A., Piersanti, G., Kathuria, S., and Piomelli, D. (2004) Cyclohexylcarbamic acid 3′- or 4′-substituted biphenyl-3-yl esters as fatty acid amide hydrolase inhibitors: Synthesis, quantitative structure-activity relationships, and molecular modeling studies, *J. Med. Chem. 47*, 4998−5008.
22. Goparaju, S. K., Ueda, N., Yamaguchi, H., and Yamamoto, S. (1998) Anandamide amidohydrolase reacting with 2-arachidonoylglycerol, another cannabinoid receptor ligand, *FEBS Lett. 422*, 69−73.
23. Goparaju, S. K., Kurahashi, Y., Suzuki, H., Ueda, N., and Yamamoto, S. (1999) Anandamide amidohydrolase of porcine brain: cDNA cloning, functional expression and site-directed mutagenesis, *Biochim. Biophys. Acta 1441*, 77−84.
24. Di Marzo, V., Bisogno, T., Sugiura, T., Melck, D., and De Petrocellis, L. (1998) The novel endogenous cannabinoid 2-arachidonoylglycerol is inactivated by neuronal- and basophil-like cells: Connections with anandamide, *Biochem. J. 331* (Part 1), 15−19.
25. Saario, S. M., Savinainen, J. R., Laitinen, J. T., Jarvinen, T., and Niemi, R. (2004) Monoglyceride lipase-like enzymatic activity is responsible for hydrolysis of 2-arachidonoylglycerol in rat cerebellar membranes, *Biochem. Pharmacol. 67*, 1381−1387.
26. Muccioli, G. G., Xu, C., Odah, E., Cudaback, E., Cisneros, J. A., Lambert, D. M., Lopez Rodriguez, M. L., Bajjalieh, S., and Stella, N. (2007) Identification of a novel endocannabinoid-hydrolyzing enzyme expressed by microglial cells, *J. Neurosci. 27*, 2883−2889.
27. Patricelli, M. P., and Cravatt, B. F. (1999) Fatty acid amide hydrolase competitively degrades bioactive amides and esters through a nonconventional catalytic mechanism, *Biochemistry 38*, 14125−14130.
28. Saghatelian, A., Trauger, S. A., Want, E. J., Hawkins, E. G., Siuzdak, G., and Cravatt, B. F. (2004) Assignment of endogenous substrates to enzymes by global metabolite profiling, *Biochemistry 43*, 14332−14339.
29. Vandevoorde, S., Jonsson, K. O., Labar, G., Persson, E., Lambert, D. M., and Fowler, C. J. (2007) Lack of selectivity of URB602 for 2-oleoylglycerol compared to anandamide hydrolysis in vitro, *Br. J. Pharmacol. 150*, 186−191.

BI7005898